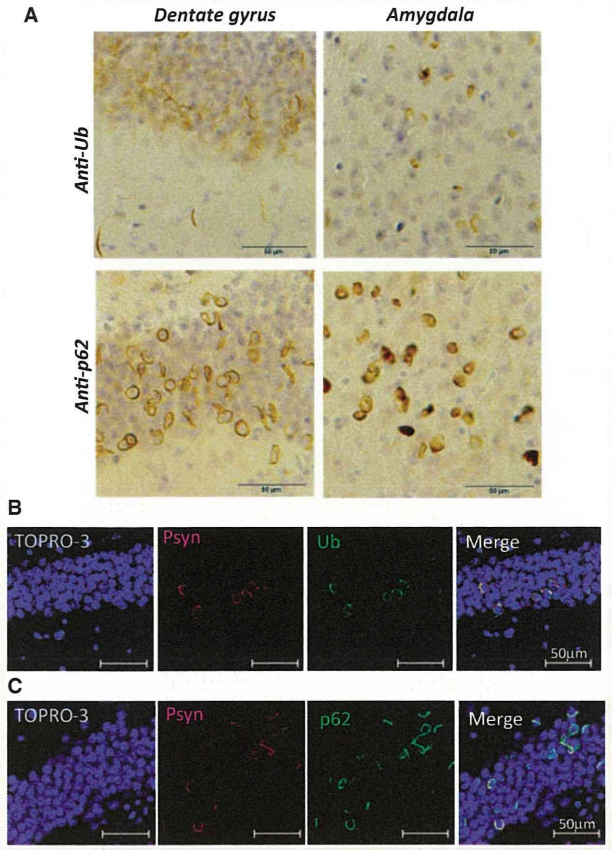

Figure 2 α-Synuclein pathology in fibril-injected mice brain was immunoreactive for ubiquitin (Ub) and p62. (**A**) Staining of dentate gyrus and amygdala of fibril-injected mice at 15 months after injection, using anti-ubiquitin (*upper*) and p62 (*lower*) antibodies. Abundant ubiquitin- and p62-positive pathology can be seen. (**B** and **C**) Double-labelled immunofluorescence of dentate gyrus for phosphorylated α-synuclein (Psyn) and ubiquitin (**B**) or p62 (**C**). Phosphorylated α-synuclein-positive structures were co-localized with ubiquitin and p62.

interestingly, anti-mouse α-synuclein strongly labelled the sarkosyl-insoluble phosphorylated α-synuclein-positive bands at Day 90, but these were not immunostained with LB509. These results clearly show that endogenous mouse α-synuclein is accumulated as phosphorylated and ubiquitinated forms. Immunohistochemical analysis with anti-tyrosine hydroxylase suggested that dopaminergic neurons are retained in substantia nigra of human α-synuclein fibril-injected mice at 6 months after injection (Fig. 5A and B). However, dramatic loss of the neurotransmitter enkephalin was observed in globus pallidus and amygdala central nucleus, where abundant phosphorylated α-synuclein-positive structures are detected (Fig. 5C and D). These data suggest that neuronal dysfunction occurs without apparent neuronal loss. We also performed behavioural analyses of mice injected with soluble human α-synuclein monomers or human α-synuclein fibrils. However, significant differences were not observed in open field test, wire hang test, rotarod test and Y-maze test (Supplementary Fig. 4) at 6 months after injection.

Next, we tested whether fibrils composed of recombinant mouse α-synuclein can induce α-synuclein pathology more efficiently than those composed of human α-synuclein, because the sequences of human and mouse α-synuclein are slightly different (Supplementary Fig. 5), and there could be a species difference. Mouse α-synuclein complementary DNA was cloned, and the protein was expressed in *Escherichia coli* and purified. Fibrils or soluble mouse α-synuclein were inoculated into substantia nigra of wild-type mouse brains and the pathology was evaluated. Strikingly, all the mice injected with mouse α-synuclein fibrils developed phosphorylated α-synuclein pathology in the injected side of the brain, whereas no pathology was detected in mice injected with soluble mouse α-synuclein (Table 2). The phosphorylated α-synuclein pathologies were basically the same as those of mice injected with human α-synuclein fibrils (data not shown). The efficiency of the induction of phosphorylated α-synuclein pathology by human α-synuclein fibrils was ~90% (Table 2), which is quite high, but slightly lower than that with mouse α-synuclein fibrils, suggesting that there may be a small species difference between mouse and human α-synuclein.

Finally, we tested whether pathological α-synuclein deposited in the brains of patients has similar prion-like properties in brains of wild-type mice. Surprisingly, pathological α-synuclein-enriched fractions also induced phosphorylated α-synuclein-positive pathologies in various areas of brain, including the substantia nigra, amygdala, hippocampus, striatum, hypothalamus, somatosensory area, motor cortex, piriform cortex and superior colliculus (Fig. 6). In brains of these mice, the phosphorylated α-synuclein-positive pathologies mostly resembled Lewy neurite-like structures. Lewy body-like pathology was detected only in amygdala and piriform cortex. The percentage of mice that developed phosphorylated α-synuclein pathology in the injected side of the brains was 50% in the group injected with insoluble phosphorylated α-synuclein of dementia with Lewy bodies brains, which is less than that in mice injected with recombinant α-synuclein fibrils (Table 2). Thus, these results demonstrate that inoculation of either pure synthetic recombinant α-synuclein fibrils or dementia with Lewy bodies brain extracts into wild-type mice can induce Lewy body/neurite-like phosphorylated α-synuclein pathology efficiently and reproducibly. Our results raise an important question, i.e. whether or not α-synuclein fibrils are transmissible among individuals. To test this possibility, we intranasally administered at high concentrarion of abnormal α-synuclein fibrils (preformed recombinant human or mouse α-synuclein fibrils) or the insoluble fraction from dementia with Lewy bodies brain to normal mice. However, no pS129-positive abnormal structures were detected in the brain at 21 months after the final administration (Supplementary Fig. 6), even with highly sensitive immunohistochemical staining, suggesting that the abnormal α-synuclein cannot pass through the nasal mucosa.

Discussion

In this study, we have shown that the inoculation of α-synuclein fibrils made of recombinant α-synuclein or dementia with Lewy bodies brain extracts into wild-type mouse brain is sufficient to

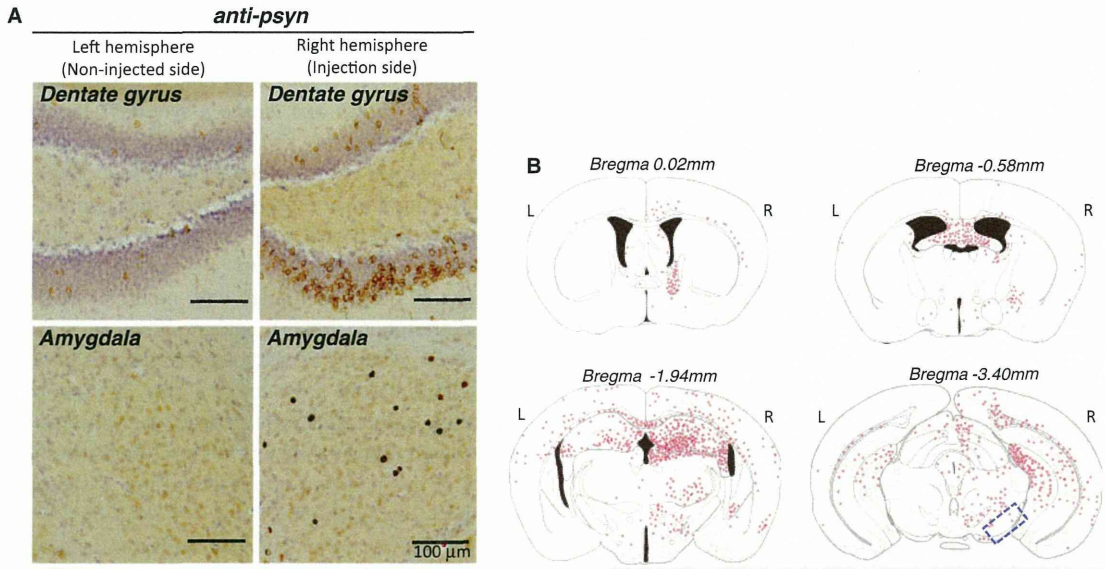

Figure 3 (**A**) Spreading of phosphorylated α-synuclein pathology on the contralateral side of mouse brain injected with α-synuclein fibrils. Staining of dentate gyrus and amygdala in the right hemisphere (injection side) and in the left hemisphere (non-injected side) with anti-phosphorylated α-synuclein (psyn) antibody, 1175, at 15 months after injection. (**B**) Distribution of phosphorylated α-synuclein pathology in human α-synuclein fibril-injected mouse brain at 15 months after injection ($n = 24$). Four coronal sections were stained with phosphorylated α-synuclein antibody, 1175. Red dots indicates Lewy bodies- and Lewy neurites-like pathology. Near the injection level (bregma -3.40 mm), abundant phosphorylated α-synuclein pathology was present in substantia nigra, hippocampus, external capsule, and entorhinal cortex in right hemisphere, whereas in the left hemisphere, sparser pathology was detected in hippocampus and external capsule. At the level of -1.94 mm from bregma, severe phosphorylated α-synuclein pathology was present in hippocampus, amygdala, corpus callosum, hypothalamus and motor, visual, somatosensory, auditory and piriform cortex in the right hemisphere, whereas moderate phosphorylated α-synuclein pathology was observed in corpus callosum, hippocampus, external capsule and motor, somasosensory and auditory cortex in the left hemisphere. At the level of -0.58 mm from bregma, phosphorylated α-synuclein pathology was detected in amygdala, corpus callosum, fimbria, fornix, hypothalamus, striatum and somatosensory and piriform cortex in the right hemisphere, whereas in the left hemisphere, the pathology was present in corpus callosum, fimbria, fornix, hypothalamus and striatum. At the level of 0.02 mm from bregma, phosphorylated α-synuclein pathology was concentrated in stria terminalis, septal nucleus and cingulate, motor and somatosensory cortex in the right hemisphere. In the left hemisphere, phosphorylated α-synuclein pathology was detected only in septal nucleus. Dashed box indicates substantia nigra (injection site). L = left hemisphere of brain; R = right hemisphere.

cause the appearance of Lewy body/neurite-like α-synuclein pathology *in vivo*. Similar work was recently published by Luk *et al.* (2012*a*) but there are important differences between our study and theirs. Luk *et al.* (2012*a*) showed that only inoculation of synthetic mouse α-synuclein fibrils into wild-type mouse brain induced synuclein pathology. In our present study, we inoculated not only fibrils made of recombinant mouse α-synuclein but also ones from human α-synuclein fibrils, and importantly also insoluble α-synuclein from dementia with Lewy bodies brains, into wild-type mouse brain. This is the first report showing efficient induction of α-synuclein pathology by inoculation of material from human brain. Furthermore, our biochemical analyses clearly demonstrate that endogenous mouse α-synuclein is converted into abnormal form and deposited in neurons of the brain through a prion-like mechanism or by seed-dependent aggregation by crossing the species barrier (Fig. 4). Since soluble α-synuclein never induced such pathology (Supplementary Fig. 2), we can conclude that the structural difference between soluble and filamentous forms of α-synuclein, i.e. cross-β structure in the α-synuclein fibrils (Serpell *et al.*, 2000) is critical for the pathogenesis. It has been reported that recombinant α-synuclein fibrils enhance the initiation and progression of α-synuclein pathology in transgenic mice overexpressing mutant α-synuclein (Mougenot *et al.*, 2012; Luk *et al.*, 2012*b*) and wild-type mice (Luk *et al.*, 2012*a*). In those models, α-synuclein pathology appeared at 90 days after inoculation. In our mouse model, abnormal phosphorylated α-synuclein pathology was also detected at 90 days after injection (Fig. 4 and Table 1), suggesting that it takes about this length of time for the formation of abnormal phosphorylated α-synuclein pathology *in vivo* after the seeding procedure. Despite a diffusion of injected exogenous α-synuclein fibrils to the bilateral sides of brain within a few hours after injection (Fig. 4), phosphorylated α-synuclein pathology seems to be initiated in the injected side and to spread from the injected side to the non-injected side in a time-dependent manner (Table 1). Thus, it is reasonable to speculate that exogenous fibrils enter neurons at the injection site as a result of infusion pressure, a temporary high concentration, or some other mechanism, and then the pathological process starts to develop from these cells.

Propagation patterns of pathology in the inoculated mice were basically identical regardless of the species of injected seeds (i.e. recombinant human α-synuclein fibrils, mouse α-synuclein fibrils or

Table 1 Semi-quantitative grading of α-synuclein pathology in mice injected with human α-synuclein fibrils

			Non-injection side (left hemisphere)			Injection side (right hemisphere)		
			Time from injection (days)			Time from injection (days)		
			90	180	450	90	180	450
Bregma	0.02 mm	Stria terminalis	–	–	–	–	+ +	+ + +
		Striatum	–	+	+	+	+ +	+ +
		Cigular cortex	–	–	–	–	+	+
		Septal nucleus	–	–	–	–	+	+
Bregma	−0.58 mm	Corpus callosum	–	–	+	–	–	+ +
		Fornix	–	+	+ +	–	+	+ +
		Hippocampal commissure	–	+	+ +	–	+	+ +
		Amygdala	–	–	–	+	+ + +	+ + +
		Globus pallidus	–	+	+	–	+	+ +
		Striatum	–	–	+	+	+	+
		Somatosensory area	–	–	+	–	+	+
		Insular cortex	–	–	–	+	+	+
Bregma	−1.94 mm	Corpus callosum	–	–	+ +	–	–	+ +
		Hippocampus	–	+	+ + +	+	+ +	+ + +
		Habenular nucleus	–	–	+	–	–	+ + +
		Fimbria	–	+	+ + +	–	+	+ + +
		Amygdala	–	–	–	+ +	+ + +	+ + +
		Hypothalamus	–	–	+	+	+	+ +
		Thalamus	–	–	–	–	–	+
		Visual cortex	–	–	+	–	+	+ +
		Somatosensory area	–	+	+	–	+	+ +
		Auditory cortex	–	–	+	+	+	+ +
		Piriform cortex	–	–	+	+	+	+ +
		External cupsule	–	–	+	–	–	+ +
Bregma	−3.40 mm	Substantia nigra	–	–	–	+	+	+
		Hippocampus	–	+	+ +	+	+ +	+ +
		Superior colliculus	–	+	+	–	+	+ +
		External cupsule	–	–	+	–	–	+
		Visual cortex	–	–	–	+	+	+
		Auditory cortex	+	+	+	+	+ +	+ +
		Entorhinal cortex	–	+	+	+	+ +	+ +

Four coronal sections were stained with anti-phosphorylated α-synuclein antibody at 90, 180 or 450 days after injection. Grading of α-synuclein pathology was performed as follows: –, none; +, slight; + +, moderate; + + +, severe. At 90 days after injection, small amounts of phosphorylated α-synuclein-positive structures were observed in substantia nigra, amygdala, striatum, hypothalamus, hippocampus, and stria terminalis in the right hemisphere of brain (injected side), but very few Lewy neurites were detected in cortex in the left hemisphere. At 180 days post-injection, the amount of phosphorylated α-synuclein-positive pathology was increased and was more widely spread in the right hemisphere, while in the left hemisphere, little phosphorylated α-synuclein pathology was apparent in hypothalamus, hippocampus, striatum or globus pallidus. At 450 days (15 months) after injection, phosphorylated α-synuclein pathology had spread throughout the right hemisphere and the left hemisphere.

dementia with Lewy bodies brain extracts), but extracts of brains with dementia with Lewy bodies showed lower propagation efficiency than recombinant fibrils (Table 2). This relatively low efficiency may be explained by the lesser amount of abnormal α-synuclein contained in the dementia with Lewy bodies brain extracts. Comparison of human α-synuclein fibrils and mouse α-synuclein fibrils indicated that mouse α-synuclein fibrils showed slightly higher efficiency (Table 2). *In vitro* experiments also indicated that mouse α-synuclein fibrils promote fibrillization of the soluble mouse α-synuclein monomer faster than human α-synuclein fibrils (Supplementary Fig. 7). It is well known that prion propagation can cross the species barrier (Prusiner, 1993) and the efficiency of propagation depends on the amino acid sequences of prion proteins. In the case of α-synuclein, mouse α-synuclein and human α-synuclein share 95% amino acid sequence homology (Supplementary Fig. 5), and this may be the reason why endogenous mouse α-synuclein is capable of aggregation by inoculation of human α-synuclein fibrils. Another factor may be that mouse α-synuclein protein has a threonine residue at amino acid position 53 (Supplementary Fig. 5), which is known as an aggregation-prone mutation in familial Parkinson's disease (Polymeropoulos *et al.*, 1997).

Time course analyses of the pathology in these mice (Table 1) showed that at 90 days after injection, phosphorylated α-synuclein pathology was mainly observed near the injection level, but also seen in striatum, amygdala, stria terminalis and dentate gyrus: areas far from the injection site had developed pathology. The striatum and the amygdala central nucleus have projections from substantia nigra, and the stria terminalis serves as a major output pathway of the amygdala (Supplementary Fig. 8). Although the

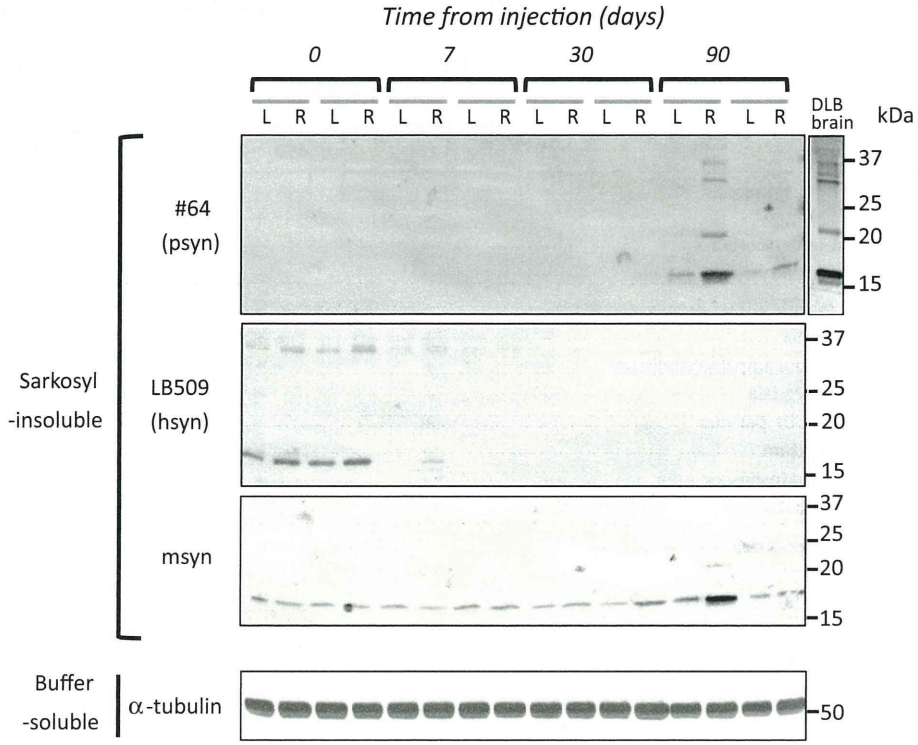

Figure 4 Endogenous mouse α-synuclein was aggregated in wild-type mouse brain injected with human α-synuclein (hsyn) fibrils. The brain was divided into two parts at the longitudinal fissure of the cerebrum. Sarkosyl-insoluble fractions were obtained from the right and left hemispheres, and analysed by immunoblotting with #64, LB509 or anti-mouse α-synuclein (msyn) antibodies. Representative images are shown (n = 14). Sarkosyl-insoluble phosphorylated α-synuclein (psyn) started to accumulate, predominantly in the right hemisphere, at 90 days after injection. It was composed of endogenous mouse α-synuclein, not exogenous human α-synuclein.

dentate gyrus does not have direct projection to substantia nigra, regions connecting with dentate gyrus (i.e., hippocampal CA1, CA3, entorhinal cortex, fimbria, fornix and hippocampal commissure) also showed moderate pathology (Table 1). These results may indicate that α-synuclein pathology propagates unidirectionally through the neural circuit (Supplementary Fig. 8). Spread of pathology from the right hemisphere to the left hemisphere might occur via the corpus callosum, hippocampal commissure, etc., connecting with the contralateral side of the brain (Fig. 3B and Table 1). Phosphorylated α-synuclein pathology in our mouse model was mainly observed in neurons and was hardly detected in glial cells, while the band pattern of sarkosyl-insoluble phosphorylated α-synuclein in mice was indistinguishable from that of dementia with Lewy bodies brains (Fig. 4), where phosphorylated α-synuclein pathology was mainly seen in neurons. Although the mechanism remains to be clarified, exogenous α-synuclein fibrils may enter cells through a selective mechanism(s), such as neuron-specific receptors. Alternatively, differences in expression levels of endogenous α-synuclein or cellular environments may also be important for formation of the pathology, even if abnormal α-synuclein has already entered the cells.

Luk *et al.* (2012*a*) reported dopaminergic neuronal loss and motor dysfunction (by Rotarod test and wire hang test) in wild-type mice injected with mouse α-synuclein fibrils at 6 months after inoculation into striatum. In contrast, our human α-synuclein or mouse α-synuclein fibril-injected mice did not

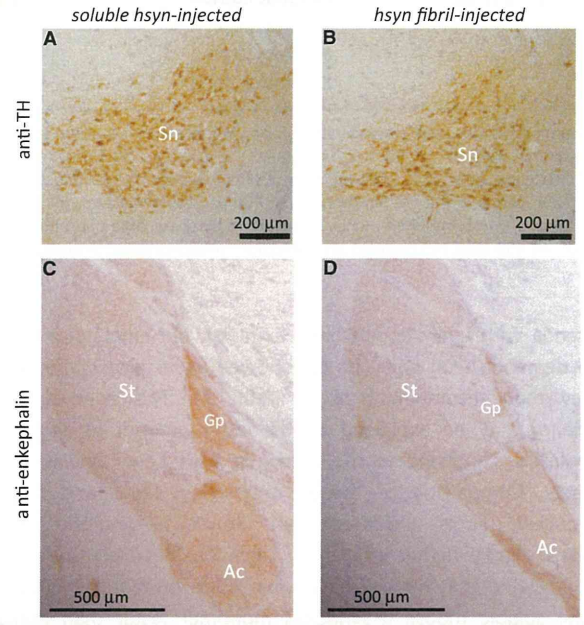

Figure 5 Fibril-injected mice show apparent reduction of a neurotransmitter enkephalin in amygdala central nucleus and globus pallidus at 15 months after injection. Brain sections were stained with anti-tyrosine hydroxylase (TH) (**A** and **B**) and anti-enkephalin (**C** and **D**) antibodies. Ac = amygdala central nucleus; Gp = globus pallidus; Sn = substantia nigra; St = striatum.

Table 2 Comparison of propagation efficiency in mice at 15 months after injection

Injection samples		Right hemisphere (injection side) anti-psyn	anti-ubiquitin	anti-p62	Left hemisphere (non-injected side) anti-psyn
Soluble human α-syn	(*n* = 8)	0/8 (0%)	0/8 (0%)	0/8 (0%)	0/8 (0%)
Insoluble human α-syn fibril	(*n* = 24)	22/24 (91.6%)	21/24 (87.5%)	22/24 (91.6%)	19/24 (79.2%)
Soluble mouse α-syn	(*n* = 4)	0/4 (0%)	0/4 (0%)	0/4 (0%)	0/4 (0%)
Insoluble mouse α-syn fibril	(*n* = 8)	8/8 (100%)	7/8 (87.5%)	8/8 (100%)	8/8 (100%)
DLB brain extracts	(*n* = 14)	7/14 (50%)	0/14 (0%)	5/14 (35.7%)	1/14 (7.1%)

In the right hemisphere, mice showing immunopositive structures for anti-phosphorylated α-synuclein (psyn), ubiquitin (Ub) or p62 were counted. In the left hemisphere, mice showing immunopositive structures for anti-phosphorylated α-synuclein were counted. Values show number of immunopositive mice/total mice, with percentage of immunopositive mice. DLB = dementia with Lewy bodies.

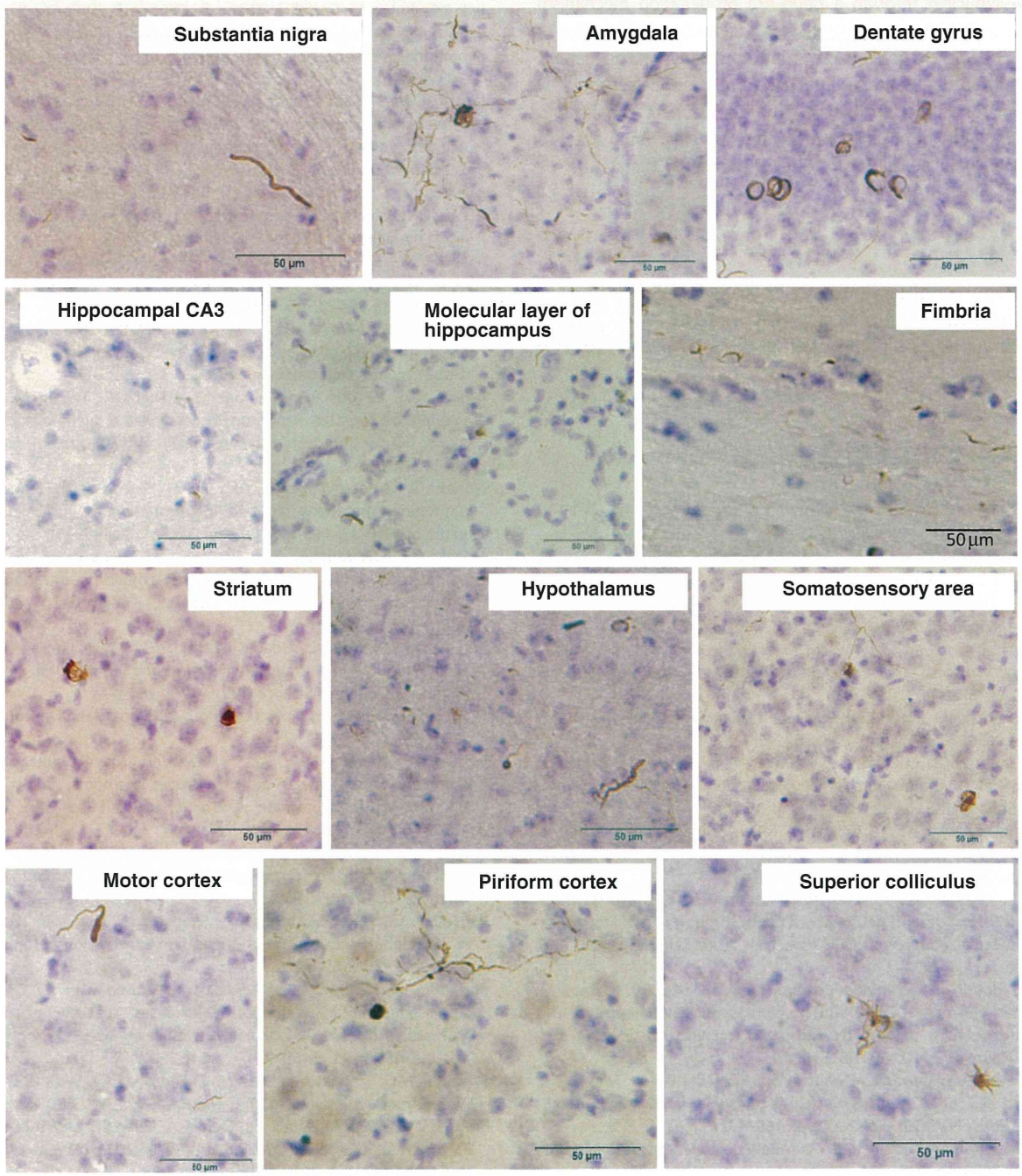

Figure 6 α-Synuclein pathology in wild-type mice brain injected with dementia with Lewy bodies-insoluble fraction observed at 15 months after injection. Sections were immunostained with anti-phosphorylated α-synuclein antibody, 1175.

show any motor and cognitive deficits at 6 months after inoculation and dopaminergic degeneration even after 15 months, a dramatic reduction of enkephalin was observed in the amygdala central nucleus and globus pallidus, with severe pathology, at 6 months after injection (Fig. 5 and Supplementary Fig. 4). The different phenotypes of these mice might be explained by differences in the injection sites [striatum in Luk *et al.* (2012*a*) and substantia nigra in our study]. Nonetheless, the spreading pattern of the pathological α-synuclein is different between our study and theirs. Differential vulnerability of neurons to these abnormal proteins may also affect phenotypes of these mice.

In summary, we have shown that intracerebral injection of insoluble α-synuclein fibrils can induce aggregation of endogenous mouse α-synuclein through a prion-like propagation mechanism. Our data suggest that phosphorylated α-synuclein pathologies do not induce acute neuronal loss but induce a slow neurodegeneration by disrupting neuronal function. These models should be useful not only for elucidating the molecular mechanisms of propagation of intracellular abnormal proteins, but also for development and evaluation of disease-modifying therapy.

Funding

This work was supported by MEXT KAKENHI Grant Numbers 12937622, 12901980 (to M.H.), JSPS KAKENHI Grant Number 11024780 (to M.M-S.) and MHLW Grant Number 12946221 (to M.H.).

Supplementary material

Supplementary material is available at *Brain* online.

References

Baba M, Nakajo S, Tu PH, Tomita T, Nakaya K, Lee VM, et al. Aggregation of alpha-synuclein in Lewy bodies of sporadic Parkinson's disease and dementia with Lewy bodies. Am J Pathol 1998; 152: 879–84.

Braak H, Braak E. Neuropathological stageing of Alzheimer-related changes. Acta Neuropathol 1991; 82: 239–59.

Chartier-Harlin MC, Kachergus J, Roumier C, Mouroux V, Douay X, Lincoln S, et al. Alpha-synuclein locus duplication as a cause of familial Parkinson's disease. Lancet 2004; 364: 1167–9.

Clavaguera F, Bolmont T, Crowther RA, Abramowski D, Frank S, Probst A, et al. Transmission and spreading of tauopathy in transgenic mouse brain. Nat Cell Biol 2009; 11: 909–13.

Desplats P, Lee HJ, Bae EJ, Patrick C, Rockenstein E, Crews L, et al. Inclusion formation and neuronal cell death through neuron-to-neuron transmission of alpha-synuclein. Proc Natl Acad Sci USA 2009; 106: 13010–5.

Emmanouilidou E, Melachroinou K, Roumeliotis T, Garbis SD, Ntzouni M, Margaritis LH, et al. Cell-produced alpha-synuclein is secreted in a calcium-dependent manner by exosomes and impacts neuronal survival. J Neurosci 2010; 30: 6838–51.

Fujiwara H, Hasegawa M, Dohmae N, Kawashima A, Masliah E, Goldberg MS, et al. Alpha-Synuclein is phosphorylated in synucleinopathy lesions. Nat Cell Biol 2002; 4: 160–4.

Goedert M. Alpha-synuclein and neurodegenerative diseases. Nat Rev Neurosci 2001; 2: 492–501.

Ibanez P, Bonnet AM, Debarges B, Lohmann E, Tison F, Pollak P, et al. Causal relation between alpha-synuclein gene duplication and familial Parkinson's disease. Lancet 2004; 364: 1169–71.

Kordower JH, Chu Y, Hauser RA, Freeman TB, Olanow CW. Lewy body-like pathology in long-term embryonic nigral transplants in Parkinson's disease. Nat Med 2008; 14: 504–6.

Kruger R, Kuhn W, Muller T, Woitalla D, Graeber M, Kosel S, et al. Ala30Pro mutation in the gene encoding alpha-synuclein in Parkinson's disease. Nat Genet 1998; 18: 106–8.

Kuusisto E, Salminen A, Alafuzoff I. Ubiquitin-binding protein p62 is present in neuronal and glial inclusions in human tauopathies and synucleinopathies. Neuroreport 2001; 12: 2085–90.

Li JY, Englund E, Holton JL, Soulet D, Hagell P, Lees AJ, et al. Lewy bodies in grafted neurons in subjects with Parkinson's disease suggest host-to-graft disease propagation. Nat Med 2008; 14: 501–3.

Luk KC, Kehm V, Carroll J, Zhang B, O'Brien P, Trojanowski JQ, et al. Pathological alpha-synuclein transmission initiates Parkinson-like neurodegeneration in nontransgenic mice. Science 2012a; 338: 949–53.

Luk KC, Kehm VM, Zhang B, O'Brien P, Trojanowski JQ, Lee VM. Intracerebral inoculation of pathological alpha-synuclein initiates a rapidly progressive neurodegenerative alpha-synucleinopathy in mice. J Exp Med 2012b; 209: 975–86.

Masuda M, Dohmae N, Nonaka T, Oikawa T, Hisanaga S, Goedert M, et al. Cysteine misincorporation in bacterially expressed human alpha-synuclein. FEBS Lett 2006a; 580: 1775–9.

Masuda M, Suzuki N, Taniguchi S, Oikawa T, Nonaka T, Iwatsubo T, et al. Small molecule inhibitors of alpha-synuclein filament assembly. Biochemistry 2006b; 45: 6085–94.

Mougenot AL, Nicot S, Bencsik A, Morignat E, Verchere J, Lakhdar L, et al. Prion-like acceleration of a synucleinopathy in a transgenic mouse model. Neurobiol Aging 2012; 33: 2225–8.

Muller CM, de Vos RA, Maurage CA, Thal DR, Tolnay M, Braak H. Staging of sporadic Parkinson disease-related alpha-synuclein pathology: inter- and intra-rater reliability. J Neuropathol Exp Neurol 2005; 64: 623–8.

Nonaka T, Kametani F, Arai T, Akiyama H, Hasegawa M. Truncation and pathogenic mutations facilitate the formation of intracellular aggregates of TDP-43. Hum Mol Genet 2009; 18: 3353–64.

Nonaka T, Watanabe ST, Iwatsubo T, Hasegawa M. Seeded aggregation and toxicity of {alpha}-synuclein and tau: cellular models of neurodegenerative diseases. J Biol Chem 2010; 285: 34885–98.

Polymeropoulos MH, Lavedan C, Leroy E, Ide SE, Dehejia A, Dutra A, et al. Mutation in the alpha-synuclein gene identified in families with Parkinson's disease. Science 1997; 276: 2045–7.

Prusiner SB. Genetic and infectious prion diseases. Arch Neurol 1993; 50: 1129–53.

Serpell LC, Berriman J, Jakes R, Goedert M, Crowther RA. Fiber diffraction of synthetic alpha-synuclein filaments shows amyloid-like cross-beta conformation. Proc Natl Acad Sci USA 2000; 97: 4897–902.

Shiotsuki H, Yoshimi K, Shimo Y, Funayama M, Takamatsu Y, Ikeda K, et al. A rotarod test for evaluation of motor skill learning. J Neurosci Methods 2010; 189: 180–5.

Singleton AB, Farrer M, Johnson J, Singleton A, Hague S, Kachergus J, et al. alpha-Synuclein locus triplication causes Parkinson's disease. Science 2003; 302: 841.

Spillantini MG, Crowther RA, Jakes R, Hasegawa M, Goedert M. alpha-Synuclein in filamentous inclusions of Lewy bodies from Parkinson's disease and dementia with lewy bodies. Proc Natl Acad Sci USA 1998; 95: 6469–73.

Spillantini MG, Schmidt ML, Lee VM, Trojanowski JQ, Jakes R, Goedert M. Alpha-synuclein in Lewy bodies. Nature 1997; 388: 839–40.

Stohr J, Watts JC, Mensinger ZL, Oehler A, Grillo SK, Dearmond SJ, et al. Purified and synthetic Alzheimer's amyloid beta (Abeta) prions. Proc Natl Acad Sci USA 2012; 109: 11025–30.

Volpicelli-Daley LA, Luk KC, Patel TP, Tanik SA, Riddle DM, Stieber A, et al. Exogenous alpha-synuclein fibrils induce Lewy body pathology leading to synaptic dysfunction and neuron death. Neuron 2011; 72: 57–71.

Wakabayashi K, Yoshimoto M, Tsuji S, Takahashi H. Alpha-synuclein immunoreactivity in glial cytoplasmic inclusions in multiple system atrophy. Neurosci Lett 1998; 249: 180–2.

Yonetani M, Nonaka T, Masuda M, Inukai Y, Oikawa T, Hisanaga S, et al. Conversion of wild-type alpha-synuclein into mutant-type fibrils and its propagation in the presence of A30P mutant. J Biol Chem 2009; 284: 7940–50.

Zarranz JJ, Alegre J, Gomez-Esteban JC, Lezcano E, Ros R, Ampuero I, et al. The new mutation, E46K, of alpha-synuclein causes Parkinson and Lewy body dementia. Ann Neurol 2004; 55: 164–73.

Cell Reports
Article

Prion-like Properties of Pathological TDP-43 Aggregates from Diseased Brains

Takashi Nonaka,[1,*] Masami Masuda-Suzukake,[1] Tetsuaki Arai,[2,3] Yoko Hasegawa,[1] Hiroyasu Akatsu,[4] Tomokazu Obi,[5] Mari Yoshida,[6] Shigeo Murayama,[7] David M.A. Mann,[8] Haruhiko Akiyama,[2] and Masato Hasegawa[1,*]
[1]Department of Neuropathology and Cell Biology
[2]Dementia Research Project
Tokyo Metropolitan Institute of Medical Science, Setagaya-ku, Tokyo 156-8506, Japan
[3]Division of Clinical Medicine, Department of Neuropsychiatry, Faculty of Medicine, University of Tsukuba, Tsukuba, Ibaraki 305-8575, Japan
[4]Choju Medical Institute, Fukushimura Hospital, Toyohashi, Aichi 441-8124, Japan
[5]Shizuoka Institute of Epilepsy and Neurological Disorders, Shizuoka, Shizuoka 420-8688, Japan
[6]Institute for Medical Science of Aging, Aichi Medical University, Nagakute, Aichi 480-1195, Japan
[7]Department of Neuropathology, Tokyo Metropolitan Institute of Gerontology, Itabashi-ku, Tokyo 173-0015, Japan
[8]Centre for Clinical and Cognitive Neuroscience, Institute of Brain Behavior and Mental Health, University of Manchester, Salford M6 8HD, UK
*Correspondence: nonaka-tk@igakuken.or.jp (T.N.), hasegawa-ms@igakuken.or.jp (M.H.)
http://dx.doi.org/10.1016/j.celrep.2013.06.007

SUMMARY

TDP-43 is the major component protein of ubiquitin-positive inclusions in brains of patients with frontotemporal lobar degeneration (FTLD-TDP) or amyotrophic lateral sclerosis (ALS). Here, we report the characterization of prion-like properties of aggregated TDP-43 prepared from diseased brains. When insoluble TDP-43 from ALS or FTLD-TDP brains was introduced as seeds into SH-SY5Y cells expressing TDP-43, phosphorylated and ubiquitinated TDP-43 was aggregated in a self-templating manner. Immunoblot analyses revealed that the C-terminal fragments of insoluble TDP-43 characteristic of each disease type acted as seeds, inducing seed-dependent aggregation of TDP-43 in these cells. The seeding ability of insoluble TDP-43 was unaffected by proteinase treatment but was abrogated by formic acid. One subtype of TDP-43 aggregate was resistant to boiling treatment. The insoluble fraction from cells harboring TDP-43 aggregates could also trigger intracellular TDP-43 aggregation. These results indicate that insoluble TDP-43 has prion-like properties that may play a role in the progression of TDP-43 proteinopathy.

INTRODUCTION

Frontotemporal lobar degeneration (FTLD) and amyotrophic lateral sclerosis (ALS) are well-known neurodegenerative disorders. FTLD is the second most common form of cortical dementia in the population below the age of 65 years (Snowden et al., 2002). ALS is the most common form of motor neuron disease and is characterized by progressive weakness and muscular wasting, and death within a few years. Ubiquitin-positive inclusions composed of misfolded proteins in neuronal and glial cells are common neuropathological features of most neurodegenerative diseases, including Alzheimer's disease (AD), Parkinson's disease (PD), FTLD, and ALS. Recently, TAR DNA-binding protein of 43 kDa (TDP-43) was identified as the major component of inclusions found in the brains of patients with ALS and FTLD (FTLD-U or FTLD-TDP) (Arai et al., 2006; Neumann et al., 2006). TDP-43, a 414-amino-acid protein expressed in nuclei, belongs to the heterogeneous ribonucleoprotein family, members of which are involved in repression of gene transcription, regulation of exon splicing, and nuclear body functions (Buratti and Baralle, 2009; Buratti et al., 2001). TDP-43 is thought to be essential for early embryonic development, because homozygous disruption of the TDP-43 gene (*TARDBP*) causes early embryonic lethality (Sephton et al., 2010; Wu et al., 2010). Interestingly, affected neurons containing cytoplasmic TDP-43 inclusions show depletion of normal nuclear TDP-43 (Arai et al., 2006; Neumann et al., 2006). Patients with these diseases show autosomal-dominant missense mutations in the *TARDBP* gene, mostly located in the C-terminal glycine-rich region (Pesiridis et al., 2009), and pathological TDP-43 is hyperphosphorylated, ubiquitinated, and abnormally cleaved to generate aggregation-prone C-terminal fragments (CTFs) (Arai et al., 2010; Hasegawa et al., 2008, 2011). Thus, loss of normal function of nuclear TDP-43 due to cytoplasmic mislocalization, and toxic gain of function due to cytoplasmic TDP-43 aggregation are potential disease mechanisms (Arai et al., 2006; Neumann et al., 2006).

Aberrant protein aggregates in affected neurons are well-known hallmarks of neurodegenerative diseases, but the mechanisms involved remain unclear. Recent reports suggest that prion-like propagation of protein aggregates composed of tau- or α-synuclein may be involved in progression of neurodegenerative diseases such as AD or PD. This is consistent with findings that tau- or α-synuclein pathology spreads in a

stereotypical temporal and topological manner (Braak and Braak, 1991; Braak et al., 2003). Furthermore, fetal mesencephalic grafts in the striatum of PD patients eventually develop Lewy bodies, suggesting that pathologic α-synuclein could be transmitted from diseased striatal neurons to grafted neurons (Kordower et al., 2008; Li et al., 2008). Cell-cell transmission of tau- and α-synuclein aggregates has been observed in both cell culture and animal models (Clavaguera et al., 2009; de Calignon et al., 2012; Desplats et al., 2009; Frost et al., 2009; Goedert et al., 2010; Liu et al., 2012; Luk et al., 2009, 2012a, 2012b; Nonaka et al., 2010; Masuda-Suzukake et al., 2013). Therefore, prion-like propagation of aberrant protein aggregates may be involved in the pathogenesis of neurodegenerative diseases.

Here, we show that insoluble TDP-43 aggregates in brains of ALS and FTLD-TDP patients have prion-like properties, including the ability to seed intracellular TDP-43 aggregation, stability against heat and proteinases, and cell-to-cell transmissibility.

RESULTS

Intracellular TDP-43 Is Aggregated in a Seed-Dependent Manner

The C-terminal portion of TDP-43 has sequence similarity to prion (Guo et al., 2011). Therefore, to investigate whether intracellular TDP-43 is aggregated in a self-templating manner, like prion, we first established a cell culture model for seeded aggregation of intracellular TDP-43 using SH-SY5Y and 293T cells (Figures 1 and S1A).

We examined whether TDP-43 forms intracellular aggregates in the presence of insoluble TDP-43 prepared from ALS or FTLD-TDP brains as seeds. We observed filamentous structures that were positive for antiphospho TDP-43 (anti-pS409/410) antibody (10–15 nm in diameter) by electron microscopy analyses of insoluble TDP-43 from brains of patients (Figure 1A). Furthermore, it was recently reported that TDP-43 inclusions in ALS and FTLD-TDP showed thioflavin positivity (Bigio et al., 2013). These results clearly indicate that insoluble TDP-43 from brains, used as seeds, had the properties of amyloid. To distinguish plasmid-derived TDP-43 from insoluble TDP-43 introduced as seeds, we used a plasmid encoding hemagglutinin (HA)-tagged TDP-43. SH-SY5Y cells were transiently transfected with HA-tagged TDP-43 and then transduced with or without N-lauroylsarcosine sodium salt (sarkosyl)-insoluble fraction (Sar-ppt) prepared from the brains of ALS (ALS ppt) or FTLD-TDP (FTLD ppt) patients. Cell lysates were fractionated and immunoblotted with anti-HA and anti-pS409/410 antibodies. In cells transfected with HA-TDP-43 plasmid alone, expressed HA-TDP-43 was detected in all fractions with an antibody against HA, whereas phosphorylated HA-TDP-43 was modestly detected in the insoluble fraction (ppt), indicating that the transiently expressed HA-TDP-43 was slightly aggregated (Figure 1B). In cells treated with ALS ppt (5 μg) alone, several bands were detected in ppt fractions with anti-pS409/410, suggesting that endogenous TDP-43 is aggregated in the presence of seeds. On the other hand, in HA-TDP-43-expressing cells transduced with ALS ppt (5 μg), bands with slower mobility were seen with an antibody against HA, and both phosphorylated full-length HA-TDP-43 and its CTFs were detected with anti-pS409/410. We confirmed that plasmid-derived TDP-43, but not ALS ppt seeds, is mainly aggregated in ppt fractions, because no bands were detected with anti-pS409/410 when ALS ppt (5 μg, used as seeds) alone was loaded on the gel (Figure 1C, rightmost lane). Similarly, full-length HA-TDP-43 and CTFs positive for anti-pS409/410 were produced in cells transfected with both HA-TDP-43 plasmid and FTLD ppt (Figures 1B and S1B). Given that plasmid-derived, nontagged TDP-43 was accumulated intracellularly in the presence of ALS ppt (Figure 1C), we mainly used a plasmid encoding, nontagged TDP-43 in subsequent work.

To test whether insoluble TDP-43 in diseased brain extracts can function as seeds for aggregation, we prepared immunodepleted ALS ppt (Figure 1D) as seeds for intracellular TDP-43 aggregation. Sar-ppt of ALS brain was incubated with a mixture of anti-TDP-43 (polyclonal; Proteintech) and anti-pS409/410 antibodies, followed by addition of protein G-Sepharose. After overnight incubation, the supernatant fraction was analyzed by immunoblotting. As shown in Figure 1D (left panel), the immunoreactivity against anti-pS409/410 found in nontreated ALS ppt was wholly lost after immunodepletion (ID). Then, we introduced immunodepleted ALS ppt (ALS ppt ID) into cells expressing HA-TDP-43, using MultiFectam. As shown in Figure 1D (right panel), the band intensities of phosphorylated full-length HA-TDP-43 and CTFs in the ppt fraction of cells expressing HA-TDP-43 and treated with ALS ppt ID were much weaker than those in the case of cells expressing HA-TDP-43 and treated with nonimmunodepleted ALS ppt. We also tested the specificity of ALS ppt as seeds for aggregation of TDP-43. When recombinant α-synuclein fibrils were introduced into cells transiently expressing α-synuclein, phosphorylated α-synuclein was accumulated in Triton-insoluble fractions (Figure S2A), as previously reported (Nonaka et al., 2010). However, intracellular α-synuclein aggregation was not observed in cells expressing α-synuclein and treated with ALS ppt (Figure S2B). Furthermore, HA-TDP-43 was not aggregated in the presence of α-synuclein fibril seeds (Figure S2C). These results showed that insoluble TDP-43 functions specifically as seeds for intracellular aggregation of TDP-43, but not for aggregation of α-synuclein.

We performed immunocytochemical analyses of cells expressing HA-TDP-43 and treated with or without ALS ppt. No phosphorylated and aggregated TDP-43 was seen in cells expressing HA-TDP-43 only (Figure 1E). A few dot-like structures positive for anti-pS409/410 were found in nontransfected cells treated with ALS ppt. On the other hand, round cytoplasmic inclusions of TDP-43 positive for both anti-pS409/410 and an antibody against Ub were detected in cells expressing HA-TDP-43 and treated with ALS ppt. The percentage of HA-positive cells that were also positive for anti-pS409/410 antibody was calculated to be 11.4% ± 4.3%. Interestingly, the immunoreactivity of an antibody against HA in nuclei of cells with cytoplasmic TDP-43 aggregates was less than that in nuclei of cells expressing HA-TDP-43 without aggregates (Figure 1E, lower left), as seen for pathogenic neurons with cytoplasmic TDP-43 inclusions in ALS and FTLD-TDP brains. Taken together, these results suggest that intracellular TDP-43 was efficiently aggregated in cultured cells in a manner that depended on seeding with insoluble TDP-43 derived from patients' brains.

Cell PRESS
Open ACCESS

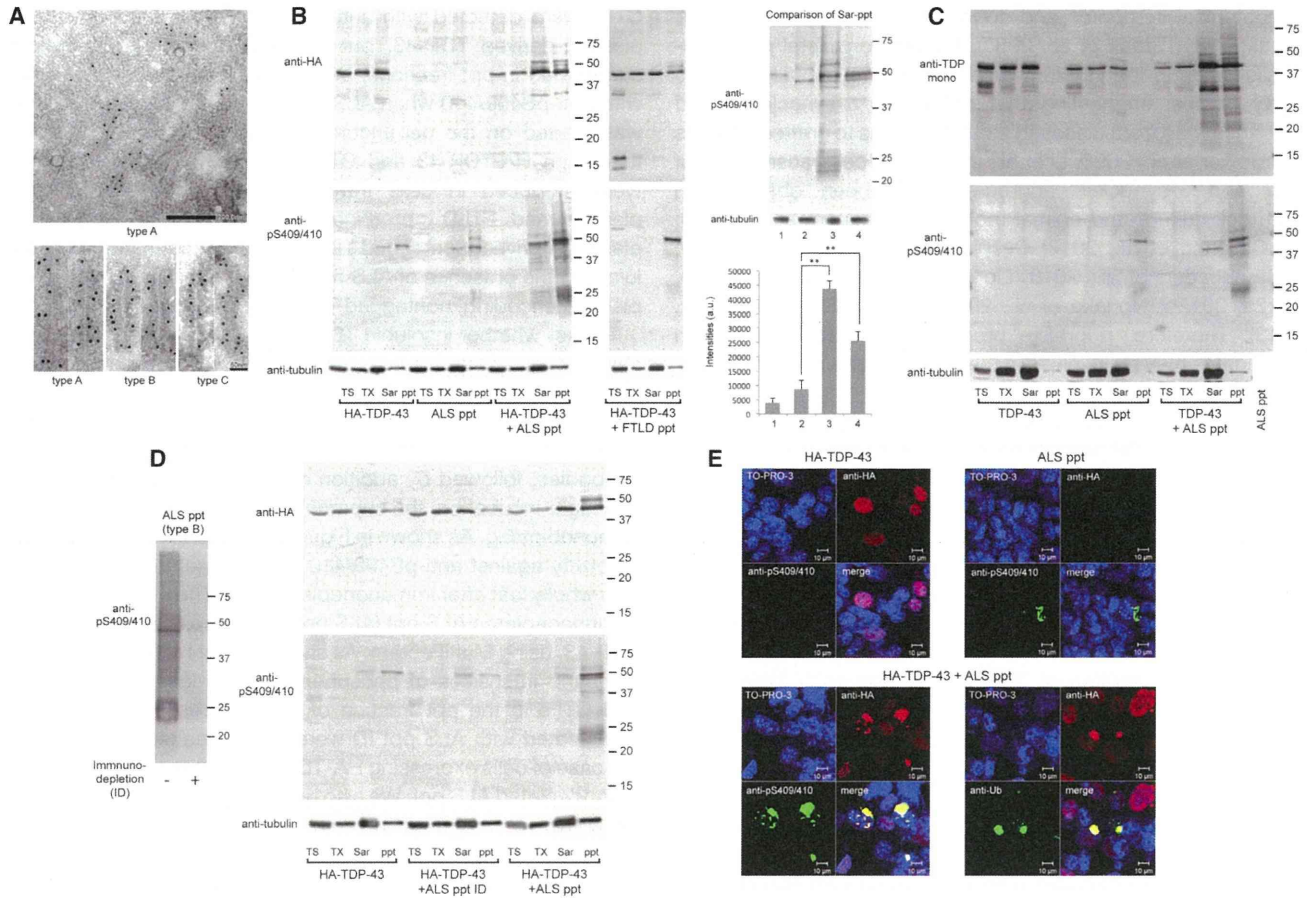

Figure 1. Detergent-Insoluble Fractions from ALS and FTLD-TDP Brains Function as Seeds for Intracellular Aggregation of Plasmid-Derived TDP-43

(A) Immuno-electron microscopy analyses of insoluble fractions from diseased brains (types A, B, and C). Filamentous structures are labeled with anti-phospho TDP-43 antibody (pS409/410). Scale bars represent 200 nm in upper panel, 50 nm in lower panel.

(B) Immunoblot analysis of lysates from cells expressing HA-TDP-43 plasmid only (HA-TDP-43), cells treated with ALS ppt (5 μg; ALS ppt), cells transfected with both HA-TDP-43 and ALS ppt (HA-TDP-43 + ALS ppt), and cells transfected with both HA-TDP-43 and FTLD ppt (5 μg; HA-TDP-43 + FTLD ppt). Proteins were differentially extracted from cells with Tris-HCl (TS), Triton X-100 (TX), and sarkosyl (Sar), leaving the pellet (ppt). Blots were probed using anti-HA (upper) and anti-pS409/410 (lower). In the right panel, the Sar-ppt fractions are shown side by side. 1: HA-TDP-43; 2: ALS ppt; 3: HA-TDP-43 + ALS ppt; 4: HA-TDP-43 + FTLD ppt. The immunoreactivity of each lane that was positive for anti-pS409/410 was quantified and the results are expressed as means + SEM (n = 3). **$p < 0.0005$ by Student's t test; a.u., arbitrary unit.

See also Figure S1.

(C) Immunoblot analysis of proteins extracted from cells expressing only nontagged TDP-43 plasmid (TDP-43), cells treated only with ALS ppt (ALS ppt), and cells transfected with both TDP-43 and ALS ppt (TDP-43 + ALS ppt). Blots were probed using anti-TDP-43 monoclonal antibody (upper) and anti-pS409/410 (lower). No bands were detected when only ALS ppt (5 μg) used as seeds was loaded on the gel (rightmost lane).

(D) ID of ALS ppt was performed with (+) or without (−) a mixture of anti-TDP-43 and anti-pS409/410 antibody. This was followed by immunoblot analyses with anti-pS409/410 (left panel). Proteins differentially extracted from cells expressing only HA-TDP-43 plasmid (HA-TDP-43), and cells transfected with both HA-TDP-43 and immunodepleted ALS ppt (HA-TDP-43 + ALS ppt ID) or untreated ALS ppt (HA-TDP-43 + ALS ppt) were analyzed. Blots were probed using anti-HA (upper) and anti-pS409/410 (lower).

(E) Confocal laser microscopy analyses of cells expressing only HA-TDP-43 plasmid (HA-TDP-43), cells treated with detergent-insoluble fraction of ALS brain (ALS ppt), and cells transfected with both HA-TDP-43 and ALS ppt (HA-TDP-43 + ALS ppt) immunostained with anti-HA (red), anti-pS409/410 (green) or anti-Ub (green), and counterstained with TO-PRO-3 (blue). Scale bars represent 10 μm.

Aggregation of Full-Length TDP-43 Precedes Generation of TDP-43 CTFs

To further investigate the seed-dependent intracellular aggregation of TDP-43, we performed time-course experiments and immunoblot analyses during TDP-43 aggregate formation. Cells expressing HA-TDP-43 and treated with or without ALS ppt were incubated for 1–3 days, and each day the cell lysates were fractionated as described above. No band positive for anti-pS409/410 was detected in any fraction on day 1 or day 2, whereas a weak band of phosphorylated HA-TDP-43 was seen in the insoluble fraction (ppt) on day 3 of cells expressing HA-TDP-43 (Figure 2A). When cells were transfected with both HA-TDP-43